Photoluminescent Nanoparticles

DOI: 10.1002/ange.200901750

Synthesis and Characterization of a Photoluminescent Nanoparticle Based on Fullerene–Silica Hybridization**

Jinyoung Jeong, Miyoung Cho, Yong Taik Lim, Nam Woong Song, and Bong Hyun Chung**

Fluorescent particles are of great interest in biotechnology for use as probes for bioimaging, diagnosis, and drug delivery in vivo or in vitro. For instance, fluorescent semiconductor quantum dots have been widely used because of their broad absorption, narrow photoluminescence (PL), and high photostability.[1] Fluorescent silica nanoparticles (SNPs) have also been developed with enhanced fluorescence and improved photobleaching for biological applications.[2] Recently, carbon-based fluorescent materials, such as carbon nanoparticles[3] and carbogenic quantum dots,[4] have been investigated as alternative fluorescent nanomaterials. By varying their size or charge, these nanomaterials exhibit multicolor coding fluorescence. Herein, we report a new platform of fluorescent nanoparticles based on a fullerene–silica hybrid prepared by a reverse microemulsion method. The fullerene–silica nanoparticles (FSNPs) are of uniform size, simple to prepare, and exhibit bright PL, high photostability, easy penetration into live cells, and low cytotoxicity, all of which are essential properties for biological applications.

Fullerenes have been explored for decades for applications in optoelectronic devices and drug-delivery systems owing to their unique structural, optical, and electrical properties.[5] Because of difficulties such as the low solubility and easy aggregation of fullerenes, these applications require functionalization with organic/inorganic composites including polymers, metals, and ceramics.[6–9] In this work, a reverse microemulsion method with a nonionic surfactant was used, for the first time, to form fullerene–silica hybrid materials (Figure 1a). C_{60} fullerenes were encapsulated in a microemulsion with the help of the cosurfactant *n*-hexanol, and were then incorporated into the silica network by the addition of triethyl orthosilicate (TEOS) as a silica precursor and ammonium hydroxide (NH_4OH) as a catalyst.[10] The scanning

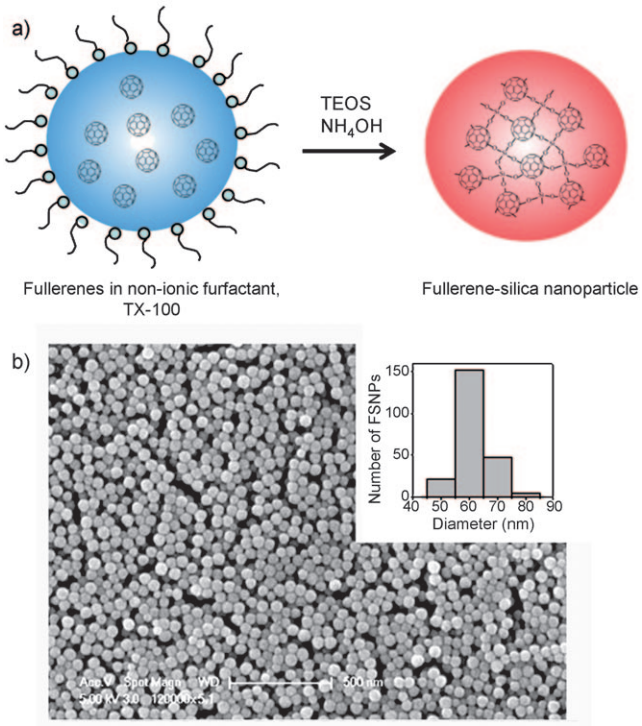

Figure 1. a) Schematic diagram of the synthesis of FSNPs. b) SEM image of as-prepared FSNPs. Inset: size distribution of the FSNPs.

electron microscopy (SEM) image in Figure 1b shows that the FSNPs are spherical and monodisperse, with an average diameter of (61.5 ± 6.0) nm (for 226 samples).

Under excitation by laser light at 488 nm, the FSNP solution showed a strong and moderately broad PL spectrum centered at 600 nm (Figure 2a). The FSNPs exhibited blue-shifted PL compared to the fluorescence of a C_{60} film ($\lambda_{max,FL} = 720$ nm). On the other hand, no significant PL intensity was observed in the SNP solution under the same laser excitation. The PL intensity of the FSNPs increased linearly with fullerene content, as shown in the plot of PL intensity versus increasing fullerene concentration for FSNP synthesis (Figure 2b and c).

To quantify the brightness of the PL from the FSNPs, we measured the PL quantum yield and the molar extinction coefficient of the FSNP solution. The PL quantum yield of the FSNP solution was determined to be 3.5×10^{-3} for 350 nm

[*] J. Jeong, M. Cho, Dr. Y. T. Lim, Prof. B. H. Chung
BioNanotechnology Research Center, Korea Research Institute of Bioscience and Biotechnology and Nanobiotechnology Major School of Engineering, University of Science and Technology
111 Gwahangno, Yuseong, Daejeon 305-806 (South Korea)
Fax: (+82) 42-879-8594
E-mail: chungbh@kribb.re.kr
Dr. N. W. Song
Center for Nano–Bio Convergence Research, Korea Research Institute of Standards and Science and Cell Dynamics Research Center at GIST
209 Gajeong-Ro, Yuseong-Gu, Daejeon 305-340 (South Korea)
Fax: (+82) 42-868-5032
E-mail: nwsong@kriss.re.kr

[**] We acknowledge financial support from the Pioneer Research Program funded by the Ministry of Education, Science, and Technology (MEST) and the Fundamental R&D Program for Core Technology of Materials by the Ministry of Knowledge Economy (MKE), Republic of Korea.

Supporting information for this article is available on the WWW under http://dx.doi.org/10.1002/anie.200901750.

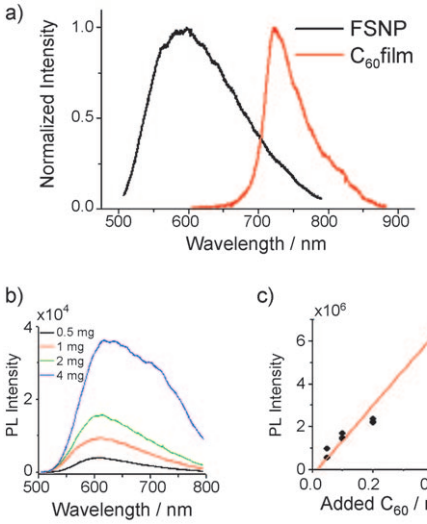

Figure 2. a) PL spectra of FSNPs and C_{60} film excited by the 488 nm Ar^+ laser line (excitation powers were 5 and 750 μW for FSNPs and C_{60} thin film, respectively). b) PL spectra of the FSNP solution with various C_{60} concentrations irradiated by 5 μW of 488 nm laser light (the concentrations of the FSNP solutions were the same). c) Integrated PL intensity of the FSNP solution with various C_{60} concentrations for FSNP synthesis.

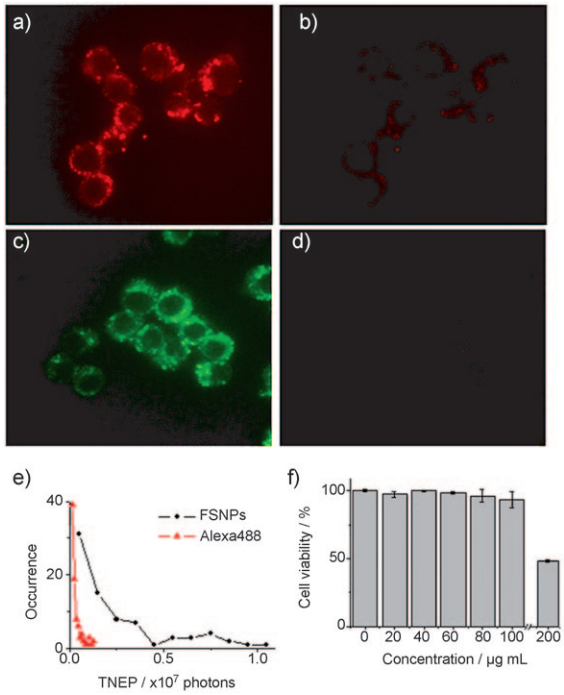

Figure 3. Photostability and cytotoxicity of the FSNPs. a) PL image of FSNPs incorporated in macrophages (RAW 264.7) under (492 ± 18) nm excitation and > 617 nm detection during the initial stage of irradiation. b) PL image of the same cells after continuous irradiation with (492 ± 18) nm light for 600 s. c) Fluorescence image of macrophage cells stained by Alexa 488-SA at the initial stage of irradiation (λ_{ex} = (492 ± 18) nm, λ_{det} > 525 nm). d) Fluorescence image of the same cells after continuous irradiation by (492 ± 18) nm light for 600 s. e) Plot of the TNEP from individual nanoparticles (FSNPs) or molecules (Alexa Fluor 488) to compare photostabilities. f) Cell viability (WST-1) assay of the FSNPs taken up by a macrophage (RAW 264.7) as a function of added particle concentration.

excitation by comparing it with the fluorescence of quinine sulfate (QS), which has a known quantum yield in 0.1 N H_2SO_4 ($\Phi_F = 0.54$).[11] This value is 35 times higher than the quantum yield of the solution containing intact fullerene ($\Phi_F = 1 \times 10^{-4}$).[12] The molar extinction coefficient of the FSNP was determined to be $3.4 \times 10^8\,M^{-1}cm^{-1}$ at 350 nm from the measured absorbance and estimated concentration of the FSNP solution, by assuming that each FSNP is a 61-nm sphere with the same density as silica ($2.2\,g\,cm^{-3}$). This value corresponds to an absorption cross section of $5.6 \times 10^8\,cm^2$, which is about 600 times larger than that of a fullerene molecule. Because the FSNP has a large absorption cross section, the PL intensity from a single FSNP is very high. From the product of the absorption cross section and the PL quantum yield, a single FSNP is estimated to be 2.1×10^4 times brighter than a single fullerene molecule when excited by 350 nm light. A single FSNP is also 400 times brighter than a single QS dye molecule under 350 nm excitation and ten times brighter than an Alexa Fluor 488 dye molecule under 494 nm excitation. Because this new photoluminescent material is on the nanometer scale, this particle is expected to play an important role in bioassays, in which very small quantities of molecules or particles must be detected.

To assess the prospects of FSNPs as a bioimaging material, we tested their photostability, cell permeability, and cytotoxicity. We observed the PL image of the FSNPs in macrophage (RAW 264.7) cells, human epithelial carcinoma cells (HeLa), estrogen receptor negative cells (SKBr3), and human umbilical endothelial cells (HUVEC) by treating them with 40–160 $\mu g\,mL^{-1}$ (0.24–0.96 nM) FSNP solutions (Figure 3 a,b and Figures S1 and S2 in the Supporting Information). Confocal PL images of the cells were analyzed by 4′,6-diamidino-2-phenylindole (DAPI) staining to identify the nuclear regions. As shown in Figure 3 a and b, the bright red spots indicating FSNPs were observed with 492 nm excitation and detection of PL at a wavelength greater than 617 nm. FSNPs were efficiently incorporated into RAW 264.7 and HeLa cells in all concentration ranges of FSNP solutions tested. Moderate internalization of FSNPs into SKBr3 and HUVEC cells was observed at the concentration range of 80–160 $\mu g\,mL^{-1}$ (0.48–0.96 nM). The photoluminescent spots were observed only in the cytoplasmic area of the cell, and the PL intensity at the central region corresponding to the nucleus was very weak. Confocal section images on the FSNP-incorporated cells also exhibited higher PL in the cytoplasmic region (Supporting Information, Figure S3). The PL images of the FSNPs were dimmer at both (upper and lower) sides of the cell membrane than those at the cell center, where the DAPI images for nuclei were also bright. These results indicate that the FSNPs easily penetrated the cell but did not enter the nuclei. This is consistent with the results of previous studies on the interaction of living cells with nanomaterials, in which genetic disruption did not occur.

As a comparative analysis, Alexa 488-labeled streptavidin (Alexa 488-SA) in the concentration range of 8–32 $\mu g\,mL^{-1}$ (730–3000 nM) was used for cell staining. As shown in

Figure S1b in the Supporting Information, Alexa 488-SA was efficiently incorporated only into the RAW 264.7 cells, which are phagocytic cells. Moderate cell incorporation was observed with HeLa cells, and a very low degree of incorporation occurred with SKBr3 and HUVEC cells, but only at a very high concentration (3000 nM). This comparative study showed that the FSNPs exhibited better cell permeability than Alexa 488-SA, and this would allow for efficient cell imaging in the cytoplasmic region.

Continuous excitation by light during cell imaging revealed a high photostability of the FSNPs in the cytoplasmic region of the cells. When cells stained with FSNP solution (Figure 3a,b) or Alexa Fluor 488 (Figure 3c,d) were continuously irradiated by 492 nm light, the fluorescence image produced by the Alexa Fluor 488 dye completely disappeared after 10 min, whereas the PL image of the FSNP-incorporated cells still exhibited moderate intensity. This result indicates that the FSNPs in live cells have a higher photostability than Alexa Fluor 488, which is considered a superior alternative to fluorescein owing to its brightness and photostability.

The photostability of FSNPs was quantitatively compared to that of Alexa Fluor 488 by using a single-molecule detection technique.[13] The total numbers of emitted photons (TNEP) from individual FSNPs and from the Alexa dye were measured and compared. For this experiment, every photoluminescent spot was continuously irradiated with 488 nm laser light, and the PL intensity was monitored until it dropped to background fluorescence levels. Then, the background fluorescence was subtracted and the PL intensity over time was integrated quantitatively. A plot of occurrence versus TNEP is shown in Figure 3e. The FSNPs emitted about eight times more photons on average than Alexa Fluor 488. This result means that FSNPs are about eight times more stable than Alexa Fluor 488.

The cytotoxicity of FSNPs was tested with a water-soluble tetrazolium salt (WST-1) assay, according to the standard protocol.[14] Cell death or viability reduction was not observed after the addition of the FSNPs to the cell culture solution, up to a concentration of 100 $\mu g\,mL^{-1}$ for 3 days (Figure 3f). This result confirms a recent report that observed no significant cytotoxic effect of fluorescent SNPs at concentrations below 0.1 $mg\,mL^{-1}$.[15] Because a cell image could be clearly observed with 40 $\mu g\,mL^{-1}$ FSNP solution (Figure 3a), the assay results indicate that FSNPs can image live cells for a long period of time without causing damage. Note that the cytotoxicity of water-soluble quantum dots results in slow damage to various cells up to a concentration of 100 $\mu g\,mL^{-1}$ and that it induces cell death at a concentration of 200 $\mu g\,mL^{-1}$.[16] FSNPs are therefore a novel photoluminescent material suitable for the bioimaging of live cells. They offer high brightness, prolonged photostability, no blinking behavior, and very low cytotoxicity.

It is surprising that FSNPs emit bright PL because neither fullerene nor SNPs emit PL at a considerable intensity. To deduce the origin of the bright PL, we analyzed the chemical structure and composition of the FSNPs with several measurement techniques. We compared the absorption spectra of FSNPs and SNPs in ethanol solutions (Supporting Information, Figure S4). The absorption spectrum of the FSNP had a higher absorbance than that of the SNP over the whole wavelength region. Furthermore, absorption bands at 225, 254, and 355 nm were observed only in the FSNP absorption spectrum, although the intensities were very weak. These bands can be attributed to the incorporated fullerenes whose absorption peaks appear at 210, 254, and 326 nm in solution (Supporting Information, inset of Figure S4). The band shift indicates that the electronic energy levels of fullerene have been altered by chemical-bond changes.

The FTIR spectrum of the FSNPs exhibited absorption bands corresponding to aromatic C=C stretching (1509 cm^{-1}), C-O-Si (ν_s at 954, ν_{as} at 1070 cm^{-1}), and Si-O-Si (δ at 468, ν_s at 800, ν_{as} at 1080–1200 cm^{-1}; Supporting Information, Figure S5). Although the absorption bands associated with Si were also observed in the SNP spectra, the aromatic C=C stretching band was observed exclusively in the FSNP spectrum. In the X-ray photoelectron spectroscopic analysis, the FSNPs showed three kinds of carbon peaks: C=C–C (284.2 eV, 59%), C–O (285.9 eV, 34%), and C(O)–O (287.7 eV, 7%). The X-ray photoelectron spectrum of the SNPs also showed three carbon peaks for C=C–C (284.2 eV, 8%), C–O (285.9 eV, 64%), and C(O)–O (287.7 eV, 28%; Supporting Information, Figure S6f). In the spectra of both the FSNPs and SNPs, peaks at 104.0 (Si 2p) and 532.4 eV (O 1s) corresponding to SiO_2 were observed. We could not find any peak at 100.4 eV in the X-ray photoelectron spectrum of the FSNPs, which corresponds to the Si–C bond, meaning that the fullerenic carbon was linked to the silica network by oxide bonds such as C-O-Si.[17]

Elemental analysis (EA) was performed on the SNPs and a series of FSNPs with various amounts of added C_{60} to evaluate the fullerene content in the FSNPs. The carbon contents in FSNPs increased with the fullerene concentration in the microemulsion solution used for synthesis (Supporting Information, Figure S7a). This result demonstrated that fullerenes were incorporated into the silica network in a dose-dependent manner, although the increase of carbon content in the FSNPs was not linearly dependent on the amount of added C_{60} as in the PL intensity measurement (Figure 2c). The nonlinear dependence of carbon content on the added C_{60} might be attributable to the difference in nanostructures of carbon–oxygen–silica networks among different batches of FSNPs. To assess the structural heterogeneity of carbon–oxygen–silica networks, thermogravimetric analysis (TGA) was performed on the SNPs and the series of FSNPs (Supporting Information, Figure S7b). In the TGA graph, the SNPs lost weight at a temperature of 100 °C for water release, 453 °C for the release of unhydrolyzed ethyl groups, and 560 °C for silanol group release. From this result, the carbon content observed in the EA of SNPs could be interpreted as resulting from the unhydrolysed ethyl groups from the silica precursor. The TGA graph of the FSNPs also exhibited weight loss behavior similar to that of the SNPs below 560 °C. However, it showed an additional weight loss in the range of 580 to 1200 °C; the TGA graph for the FSNPs was stabilized over 1200 °C. This result indicates that fullerenic carbon atoms linked with silica were incorporated into the FSNPs.[18] The above results suggest that fullerene forms chemical bonds with silica through a C-O-Si linkage, which is

known to be a source of PL in the visible range.[19,20] Structural defects may form in the silicate network owing to the insertion of carbon atoms from fullerene molecules.

As the nanoparticles underwent thermal decomposition at 1000 °C during EA, we compared the weight loss up to 1000 °C with the EA results. The weight loss was greater than the carbon content, since the decrease in weight originated not only from the carbon loss but also from the loss of solvents and silanol groups. Although it was not highly linearly dependent, the increase in weight loss correlated with the increase in the amount of added C_{60} (Supporting Information, Figure S7c). Furthermore, the weight losses were linearly dependent on the carbon content obtained by EA (Supporting Information, Figure S7d). This result indicated that nanostructural variation among different batches of FSNPs gave rise to the increased uncertainty in the quantification of carbon or thermally decomposable species. Since the EA and TGA techniques used in these experiments were commonly based on thermal decomposition, the two results could be correlated with each other.

In summary, we have synthesized highly photoluminescent, fullerene-based SNPs by the reverse microemulsion method. The nanoparticles were spherical with a homogeneous diameter of ≈60 nm. These particles showed excellent properties for bioimaging applications, such as high luminescence, easy penetration into live cells, remarkable photostability, and nontoxicity to cells. The origin of red PL from the FSNPs might be defects formed in the silica network by fullerenic carbon atoms. Although defects in the silica network have previously been reported to be responsible for PL in the visible wavelength region, this result is the first to utilize the PL source as a bioprobe in the homogeneous particulate form. Because the silica surface of FSNPs can be easily modified with biomaterials, this novel material is an excellent candidate for a live-cell imaging agent.

Experimental Section

C_{60} fullerene (99%) was purchased from SES Research (Houston, TX, USA). All chemical solvents and reagents were purchased from Sigma–Aldrich (St. Louis, MO, USA).

FSNPs were synthesized by the modified reverse microemulsion method.[10] Various concentrations of C_{60} fullerene (0.5–4 mg in 2 mL toluene) were added to microemulsion solutions composed of cyclohexane (5 mL), hexanol (2 mL), distilled water (0.5 mL), and Triton X-100 (1.7 mL). The pinkish solution turned a red-brown color within 5 min after the injection of ammonium hydroxide (28 wt%, 60 μL) followed by TEOS (100 μL). The mixture was stirred for 20 h to allow nanoparticle formation. Then ethanol (20 mL) was added to stop the reaction, and the resultant particles were suspended in an ethanol solution. The nanoparticle solution was centrifuged at 10000 rpm. After removal of the supernatant, the sediment was resuspended in ethanol (20 mL) as a washing step. After two more washing steps of centrifugation, supernatant removal, and resuspension in ethanol and one washing step with water resuspension, the nanoparticles were dried overnight in an oven at 60 °C.

The size and structure of the FSNPs were analyzed by field-emission SEM (FEI, Sirion, Netherlands) and TEM (JEOL, JEM 2100F, Japan) at accelerating voltages of 5 and 200 kV, respectively. For measurement of the PL spectrum and the single-dot PL study, light at 488 nm from an Ar^+ laser (35 LAP 321, Melles Griot) was used. A detailed description of the PL setup can be found elsewhere.[13] The PL quantum yield of the FSNPs was determined by a standard procedure based on the measurement of UV/Vis absorption with a spectrophotometer (Beckman Coulter, DU-800, USA) and the PL spectra with a spectrofluorometer (Perkin–Elmer, LS55, UK). Images of live cells were acquired with a fluorescence microscope (Applied Precision, DeltaVision, USA). To obtain IR spectra, each sample was ground with KBr powder and the transmittance of each resulting pellet was measured with an FTIR spectrophotometer (Brucker Optics, IF66, USA). The high-resolution X-ray photoelectron spectra were measured by using an X-ray photoelectron spectroscope (ThermoVG, Sigma Probe, UK) with a resolution of 0.4 eV. The X-ray source was monochromatic $Al_{K\alpha}$. EA was performed with an element analyzer (Thermo Finnigan, Italy), and carbon contents were obtained by averaging the results of triplicate measurements. TGA graphs were recorded with thermogravimetric analyzers (Netzsch, TG209F3, Germany and Setsys 16/18, Setaram, France).

Received: April 1, 2009
Published online: June 16, 2009

Keywords: fullerenes · imaging agents · nanoparticles · photoluminescence · silica

[1] W. C. W. Chan, S. Nie, *Science* **1998**, *281*, 2016–2018.
[2] H. Ow, D. R. Larson, M. Srivastava, B. A. Baird, W. W. Webb, U. Wiesner, *Nano Lett.* **2005**, *5*, 113–117.
[3] H. Liu, T. Ye, C. Mao, *Angew. Chem.* **2007**, *119*, 6593–6595; *Angew. Chem. Int. Ed.* **2007**, *46*, 6473–6475.
[4] Y.-P. Sun et al., *J. Am. Chem. Soc.* **2006**, *128*, 7756–7757; see the Supporting Information.
[5] a) A. R. Kortan, N. Kopylov, S. Glarum, E. M. Gyorgy, A. P. Ramirez, R. M. Fleming, F. A. Thiel, R. C. Haddon, *Nature* **1992**, *355*, 529–532; b) L. L. Dugan, D. M. Turetsky, C. Du, D. Lobner, M. Wheeler, C. R. Almli, C. K. F. Shen, T. Y. Luh, D. W. Choi et al., *Proc. Natl. Acad. Sci USA* **1997**, *94*, 9434–9439; c) H. Isobe, W. Nakanishi, N. Tomita, S. Jinno, H. Okayama, E. Nakamura, *Mol. Pharm.* **2005**, *3*, 124–134.
[6] P. Innocenzi, G. Brusatin, *Chem. Mater.* **2001**, *13*, 3126–3139.
[7] E. A. Whitsitt, A. R. Barron, *Chem. Commun.* **2003**, 1042–1043.
[8] L. Zhu, P. P. Ong, J. Shen, J. Wang, *J. Phys. Chem. Solids* **1998**, *59*, 819–824.
[9] S. V. Patwardhan, N. Mukherjee, M. F. Durstock, L. Y. Chiang, S. J. Clarson, *J. Inorg. Organomet. Polym.* **2002**, *12*, 49–55.
[10] R. P. Bagwe, C. Yang, L. R. Hilliard, W. Tan, *Langmuir* **2004**, *20*, 8336–8342.
[11] J. W. Eastman, *Photochem. Photobiol.* **1967**, *6*, 55–72.
[12] J. W. Arbogast, A. P. Darmanyan, C. S. Foote, Y. Rubin, F. N. Diederich, M. M. Alvarez, S. J. Anz, R. L. Whetten, *J. Phys. Chem.* **1991**, *95*, 11–12.
[13] H.-H. Kim, N. W. Song, T. S. Park, M. Yoon, *Chem. Phys. Lett.* **2006**, *432*, 200–204.
[14] H. Yamawaki, N. Iwai, *Am. J. Physiol. Cell Physiol.* **2006**, *290*, C1495–C1502.
[15] Y. Jin, S. Kannan, M. Wu, J. X. Zhao, *Chem. Res. Toxicol.* **2007**, *20*, 1126–1133.
[16] A. Shiohara, A. Hoshino, K. Hanaki, K. Suzuki, K. Yamamoto, *Microbiol. Immunol.* **2004**, *48*, 669–675.
[17] W. K. Choi, T. Y. Ong, L. S. Tan, F. C. Loh, K. L. Tan, *J. Appl. Phys.* **1998**, *83*, 4968–4973.
[18] Y. Wang, D. Nepal, K. E. Geckeler, *J. Mater. Chem.* **2005**, *15*, 1049–1054.
[19] W. H. Green, K. P. Le, J. Grey, T. T. Au, M. Sailor, *Science* **1997**, *276*, 1826–1828.
[20] K. S. Kang, J. H. Kim, *J. Phys. Chem. C* **2008**, *112*, 618–620.

